Measuring *In situ* Rock Stress by means of the Compact Conical-ended Borehole Over-coring (CCBO) Technique

by

Katsuhiko Sugawara* and Yuzo Obara*
*Department of Architecture and Civil Engineering
(*Received* 15 *October* 1998)

Abstract

Compact conical-ended borehole overcoring (CCBO) is proposed for *in situ* rock stress measurement applicable to the faulted and highly jointed rock formations. Apparatus and operating procedure are described in detail. The observation equation on the stress tensor to be used in practice is presented, along with the possible ways for representing and interpreting the results. Thus, it is stated how the three dimensional state of *in situ* rock stress is determined from the strains on the conical end surface of a single borehole. The error in stress and stresses in an isotropic or transversely isotropic rock mass are obtained. Additionally, the reliability and the applicability of the present technique is successfully verified from the case studies.

1. Introduction

In situ rock stress is of prime importance for construction of such rock structures, as underground openings and tunnels, because the mechanical behavior of rock masses surrounding underground openings is dominated by rock stress, and also the stability of rock structures strongly depends upon the state of rock stress. For the rock stress measurement, various methods and devices have been developed and applied to a wide range of rock types. For example, the suggested method of the International Society for Rock Mechanics prepared by Kim and Franklin covers flatjacks, hydraulic fracturing and USBM and CSIRO overcoring [1].

It is desirable that the stress tensor can be determined from measurements in a single borehole, and that the necessary stress relieving is completed by the compact overcoring of smaller diameter. The compact conical-ended borehole overcoring (CCBO) technique proposed in the present paper is a development of the hemispherical-ended cell proposed by Sugawara et al. [2-7]. The stress tensor can be determined from the strains on the conical end surface of a single borehole, and the error in stress can be also determined. Calculation of the rock stresses from the rock strains can be conducted for isotropic and transversely isotropic rock. The necessary stress relieving is readily completed by the compact overcoring of the same diameter as the installation borehole. Continuous strain monitoring system is possible as well as the compact overcoring. In general, the cell utilizes sixteen elemental strains on the conical end surface of the borehole.

In the present paper, the theory and practice of the CCBO technique are clarified. The apparatus and operating procedure for measuring *in situ* rock stresses are described in detail, together with the data recording and reduction. Guidance is given on the number of strain gauges required for a specified accuracy. Possible ways for presenting and interpreting the results are explained. The proposed measurement is supported by case studies.

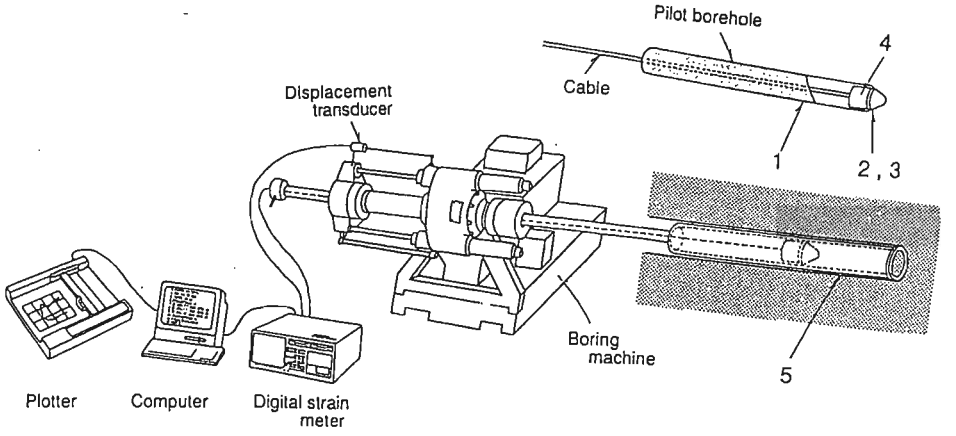

Figure 1 A schematic view of the CCBO stress measurement; 1: drilling a 76mm-diameter borehole; 2: creating a conical borehole socket; 3: borehole socket cleaning; 4: gluing the strain cell into the place; 5: compact overcoring.

2. Apparatus and Overcoring Procedure

A schematic diagram of the CCBO stress measurement is shown in **Figure 1**, and the CCBO strain cell and illustrative photographs of the components are shown in **Figure 2**. The following equipment and supplies are needed to conduct the CCBO tests:

a) Rock drill capable of drilling a 76mm-diameter borehole;
b) Diamond bit for creating conical borehole socket;
c) Forward-facing borehole camera to inspect quality of borehole socket;
d) Borehole socket cleaning materials;
e) The 16 or 24 element conical strain cell;
f) Strain cell insertion device (which includes orientational capability);
g) Electrical connection from the strain cell through the rod/water swivel;
h) 76mm-diameter diamond overcoring bit with thin-walled (3mm) barrel;
i) Displacement transducer to monitor the advance of overcoring;
j) Digital strain meter to process and record the strain cell data;
k) Computer and software to calculate stresses from strains.

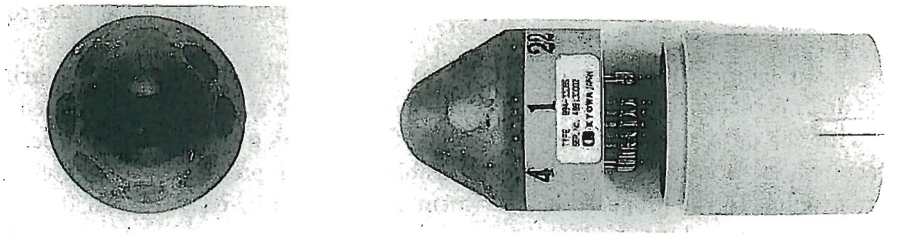

(a) (b)

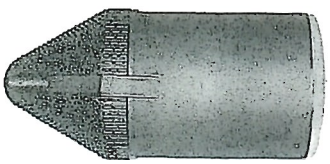

(c)

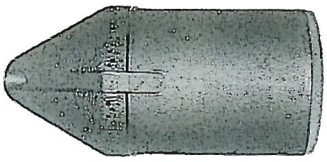

(d)

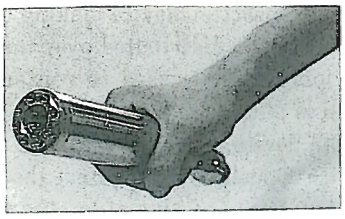

(e)

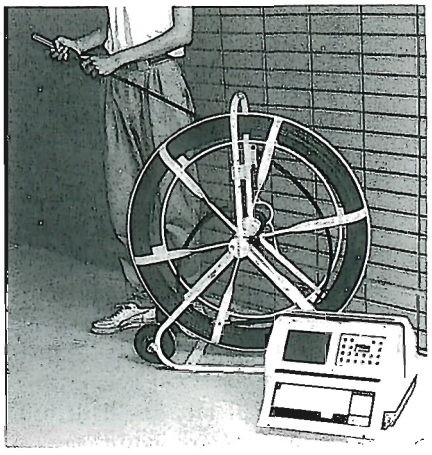

(f)

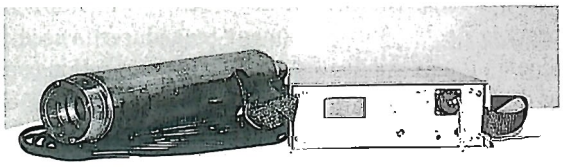

(g)

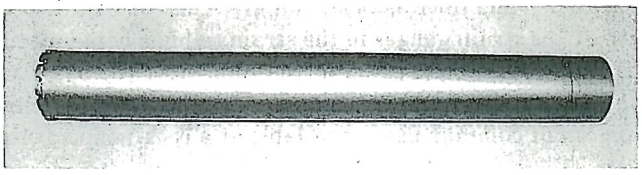

(h)

Figure 2 The CCBO strain cell and illustrative photographs of the components; (a) top view of the 24 element conical strain cell; (b) side view of the 24 element conical strain cell; (c) borz crown diamond bit; (d) impregnated diamond bit; (e) top view of forward-facing borehole camera; (f) forward-facing borehole camera system; (g) strain cell insertion device and indicator of orientation; (h) compact diamond overcoring bit with thin-walled barrel.

Rock drill capable of drilling a 76mm-diameter borehole (i.e. NX borehole) is at first required, and the initial borehole is drilled up to the required distance (the maximum is so far 40m). At the bottom of the borehole, the conical socket is created using the specified bolz and impregnated diamond bits and by applying the same drilling equipment. On completion of the borehole socket forming, a borehole camera is used to inspect the quality of the socket. The socket should appear uniform and isotropic. There should be visually no open cracks in the socket and no running water. Using the soft cloth and acetone, the surface of the borehole socket is cleaned to remove the dust particles prior to the gluing of the strain cell. On completion of the cleaning, the socket is again inspected by the borehole camera. If there still exist dust particles evidently, cleaning should be done again, until the socket becomes visually clean. Prior to installation of the strain cell, all the electrical circuits and strain gauge resistance are checked. Then the strain cell is attached to the insertion device making sure that the cable is threaded through the insertion device. The glue is then distributed over the head of the strain cell. The strain cell is then inserted in the borehole and pushed to contact to the socket. The insertion device can be rotated so that the cell is placed in the borehole socket at a specific orientation, using the inclinometer in the insertion device.

Once the orientation has been decided, the insertion device is pushed hard against the borehole socket and held firm for 30mins until the glue sets. On completion of this step, the insertion device is removed from the borehole. It is important to measure the exact distance from a point on the drilling machine to the strain cell (as a reference for the distances of the overcoring measurement). The electrical connections from the strain cell are passed through the thin walled overcoring drill bit, the drill rods, and the water swivel. The electrical circuits and strain gauge resistance are again checked, in addition to the monitoring and data logging equipment.

The overcoring is conducted using the thin walled (3mm) 76mm-diameter bit, which is of the same diameter as the borehole itself. A displacement transducer is used to monitor the advance of overcoring, which is continuously conducted until the strain cell is completely overcored over the minimum overcoring distance 100mm to about 300mm. If a joint is encountered, the strain cell/core recovery is easier. It is noted that the strain cell is not reused.

During overcoring, the data are generally recorded for every 5mm overcoring advance. When higher precision is required, the reading is made every 2mm. The data are recorded on computer disk and tabulated. In general, as a check on overcoring progress, one channel is monitored, concerning a relation of gauge output versus distance.

The equipment specification and tolerances are not given here in detail, because many of these interact and the length of the strain gauges in the strain cell has been optimized through theory and experience. Some of information is given in the references [8, 9]. The equipment can be operated easily, as mentioned above. Also, several papers have been published on its use [10, 11]. The conical strain cell of common use is available at a rock temperature range from 0℃ to 60℃.

3. Data Reduction

3.1 Principle of *in situ* rock stress determination

In situ rock stresses acting on rock mass surrounding a stress measuring station are assumed to be uniform prior to the boring, and the magnitudes of their components are calculated from the strains on a conical socket, based on the theory of elasticity [9-15].

3.2 Co-ordinates and expression of *in situ* stress tensor of rock

For calculation of *in situ* stress tensor of rock from the strains, the cylindrical co-ordinates (r, θ, z), the spherical co-ordinates (ρ, θ, φ) and the Cartesian co-ordinates (x, y, z) are defined respectively as illustrated in **Figure 3**, making the z-axis coincident with the axis of the borehole. The *in situ* stress tensor of rock $\{\sigma\}$ is expressed as follows:

$$\{\sigma\} = \{\sigma_x, \sigma_y, \sigma_z, \tau_{yz}, \tau_{zx}, \tau_{xy}\}^T \quad (1)$$

where σ_x, σ_y, σ_z, τ_{yz}, τ_{zx} and τ_{xy} are the stress components in the Cartesian co-ordinates.

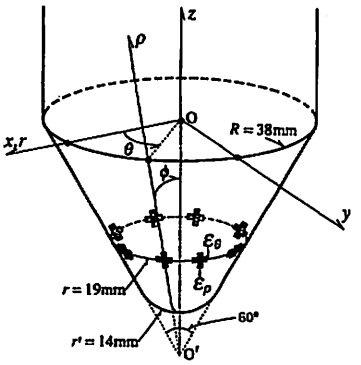

Figure 3 Co-ordinates systems fixed to the conical borehole socket and the strains to be measured by the 16 element method.

3.3 Strains to be measured

The strains are required to be measured at the specified eight points on the conical socket of 76mm diameter. These points are axisymmetrically arranged along a measuring circle of 19mm radius, by rotating 45 degrees at a step. Strain measuring points has been specified through theory and experience [9]. In the usual 16 element method, the tangential strain ε_θ and the radial strain ε_ρ are measured at each strain measuring points, using an 16 element strain cell. The 24 element method requires the additional strain at each point, that is the oblique strain ε_φ, as shown in **Figure 4**. The angle between ε_r and ε_φ is 45 degrees and that between ε_θ and ε_φ is 45 degrees. Thus, the strains measured on a conical borehole socket can be denoted by

$$\{\beta\} = \{\beta_1, \beta_2, \beta_3, \ldots, \beta_n\}^T \quad (2)$$

where n: number of strains; i.e. $n=16$ for the 16 element method: $n=24$ for the 24 element method.

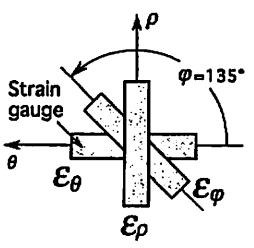

Figure 4 The strain gauge arrangement for the 24 element method.

3.4 Relations between the strains and the *in situ* stress tensor of rock

The strains $\{\varepsilon_\theta, \varepsilon_\rho, \varepsilon_\varphi\}$ at a strain measuring point of a tangential angle θ are given in the isotropic case, as follows:

$$\begin{Bmatrix}\varepsilon_\theta\\ \varepsilon_\rho\\ \varepsilon_\varphi\end{Bmatrix} = \begin{bmatrix} A_{11}+A_{13}\cos 2\theta & , A_{11}-A_{13}\cos 2\theta & , C_1,\\ A_{21}+A_{23}\cos 2\theta & , A_{21}-A_{23}\cos 2\theta & , C_2,\\ A_{31}+A_{33}\cos 2\theta+A_{32}\sin 2\theta, & A_{31}-A_{33}\cos 2\theta-A_{32}\sin 2\theta, & C_3, \end{bmatrix}$$

$$\begin{bmatrix} D_{11}\sin\theta & , D_{11}\cos\theta & , 2A_{13}\sin 2\theta\\ D_{21}\sin\theta & , D_{21}\cos\theta & , 2A_{23}\sin 2\theta\\ D_{31}\sin\theta-D_{32}\cos\theta & , D_{31}\cos\theta+D_{32}\sin\theta & , 2A_{33}\sin 2\theta-2A_{32}\cos 2\theta \end{bmatrix} \cdot \frac{\{\sigma\}}{E} \quad (3)$$

where E is the Young's modulus of rock, and A_{11}, A_{13}, ..., D_{32} are the constants and are termed as the strain coefficients.

3.5 Strain coefficients depending upon Poisson's ratio

The values of the strain coefficients are dependent upon Poisson's ratio of rock. These values have to be evaluated by the numerical analysis, since there is no analytical solution. The strain coefficients of the isotropic case computed by the BEM analysis are summarized in **Table 1.** The strain coefficients for transversely isotropic rock are given in the references [16].

Table 1 Strain coefficients in the isotropic case

Poisson's ratio	A_{11}	A_{13}	A_{21}	A_{23}	A_{31}	A_{32}	A_{33}
0.10	1.002	−1.726	0.109	0.343	0.562	−0.802	−0.724
0.20	1.000	−1.752	0.022	0.365	0.519	−0.818	−0.707
0.25	0.999	−1.733	−0.021	0.373	0.496	−0.821	−0.693
0.30	0.997	−1.704	−0.065	0.380	0.474	−0.822	−0.679
0.40	0.989	−1.611	−0.154	0.386	0.426	−0.823	−0.625

Poisson's ratio	C_1	C_2	C_3	D_{11}	D_{21}	D_{31}	D_{32}
0.10	−0.155	0.655	0.246	0.082	1.542	0.802	−1.725
0.20	−0.263	0.641	0.185	0.095	1.627	0.860	−1.860
0.25	−0.317	0.636	0.155	0.101	1.673	0.886	−1.923
0.30	−0.371	0.632	0.126	0.108	1.716	0.911	−1.983
0.40	−0.481	0.630	0.071	0.123	1.787	0.953	−2.091

Remarks: $A_{12} = A_{22} = D_{12} = D_{22} = 0$

3.6 Observation equation of the *in situ* rock stress

Observation equation of the *in situ* stress tensor $\{\sigma\}$ is expressed by the following matrix equation.

$$[A]\{\sigma\} = E \cdot \{\beta\} \tag{4}$$

where $[A]$ is an n x 6 elastic compliance matrix normalized by the Young's modulus E. The elements of $[A]$ are computed by substituting the tangential angle θ at each strain measuring point in equation (3)

3.7 The most probable values of *in situ* rock stresses

The most probable values of the rock stresses are determined by the mean square method, providing the normalized expression of equation (4) as follows:

$$[B]\{\sigma\} = E \cdot \{\beta^*\} \tag{5}$$

where $[B] = [A]^T \cdot [A]$, $\{\beta^*\} = [A]^T \cdot \{\beta\}$. The most probable values of the rock stress: $\{\sigma^*\}$ are expressed as

$$\{\sigma^*\} = E \cdot [C] \cdot \{\beta^*\} \tag{6}$$

where $[C]$ is the inverse matrix of $[B]$.

3.8 Standard deviations of the most probable values

The standard deviations ξ_i of each stress component is in general evaluated by assuming that the error of measured strain obeys the normal probability distribution, as follows:

$$\xi_i^2 = c_{ii} E^2 \xi_\beta^2, \qquad i = 1,2, \ldots, 6 \tag{7}$$

where ξ_β^2 is the variance of measured strains and c_{ii} is a corresponding diagonal element of the matrix $[C]$.

3.9 Simulation of the compact overcoring process

Equation (3) is available to describe the variation of strain during the compact overcoring. However, for the intermediate steps, when overcoring is not complete, FEM and BEM analyses are used to determine the components of the elastic compliance matrix for the different degrees of overcoring. Thus, one software is required for the process simulation [12, 14, 15].

3.10 Elevated rock temperature

In the case where the rock is of a different temperature from the overcoring drilling water, the bonded cell which initially is of the rock temperature is cooled by the drilling water. Then, the strains have to be corrected, using the coefficient of thermal expansion. It is normally essential to know the rock temperature and the coefficient of thermal expansion. This is, however, a complex subject because the correction may also depend on the length of the borehole. A compensation technique has been developed to account for the temperature effect [17]. Strain cells with a temperature sensor have been developed.

3.11 Comparison of strain sensitivity

Accuracy of the method is closely related with the strain sensitivity at strain measuring points. In other words, it is associated with the borehole geometry and strain gauge arrangement. When the observation error of strain follows the normal probability distribution as given in equation (7), the variance of each stress component is in direct proportion to the magnitude of the corresponding diagonal element c_{ii} of the matrix [C], and also to the error variance ξ_β^2 of the strain measured. In the CCBO method, the magnitude of c_{ii} is dependent upon the radius of the strain measuring circle, the number of the strain gauges and Poisson's ratio of rock. In order to improve the accuracy of the method, thus the minimization of the maximum value c_{max} of c_{ii} is required for determining the optimum strain gauge arrangement. The values of c_{max} of the CCBO method are summarized in **Table 2**, comparing with those of the conventional strain measurement overcoring methods [2, 8, 15].

The smallest value of c_{max} is obtained by the hemispherical-ended borehole technique. In the CCBO method, the value of c_{max} decreases with increasing the number of strain gauges. In the case that Poisson's ratio is 1/4, the values of c_{max} of the CCBO method are almost the same as that of the direct strain measurement by three rosette typed strain gauges on cylindrical wall of a borehole.

Table 2 Comparison of c_{max}

Method	Radius ratio of strain measuring circles: r/R	Number of strains to be measured: n	Poisson's ratio of rock: ν	Maximum value of c_{ii}: c_{max}	Remarks
The CCBO 16 element method	0.5	16	1/6 1/4 1/3	0.291 0.316 0.360	proposed
The CCBO 24 element method	0.5	24	1/6 1/4 1/3	0.248 0.262 0.289	proposed
Conical-ended borehole method	0.589	12	1/6 - 1/3	0.378 - 0.467	presented by Kobayashi et al.[21]
Hemispherical-ended borehole method	0.766	16	1/6 1/4 1/3	0.127 0.133 0.148	presented by Sugawara et al.[2]
Strain measurement on cylindrical wall of a borehole	1.0	9	1/4	0.280	using three rosette-typed strain gauges

4. Results of *in situ* observation

The evolution of the strain gauges for every 5mm (or 2mm) overcoring advance can be plotted, with the terminal strain distributions around the strain cell. **Figure 5** shows an example of the evolution of the strain gauges for every 5mm overcoring advance, comparing to the theoretical curves [12]. The lateral axis of the figure represents the overcoring advance, that is the distance in the axial direction between the head of the compact overcoring and the strain measuring circle on the conical socket. The changes in strain are rapid in all cases after the compact overcoring passed through the section of the strain measuring circle.

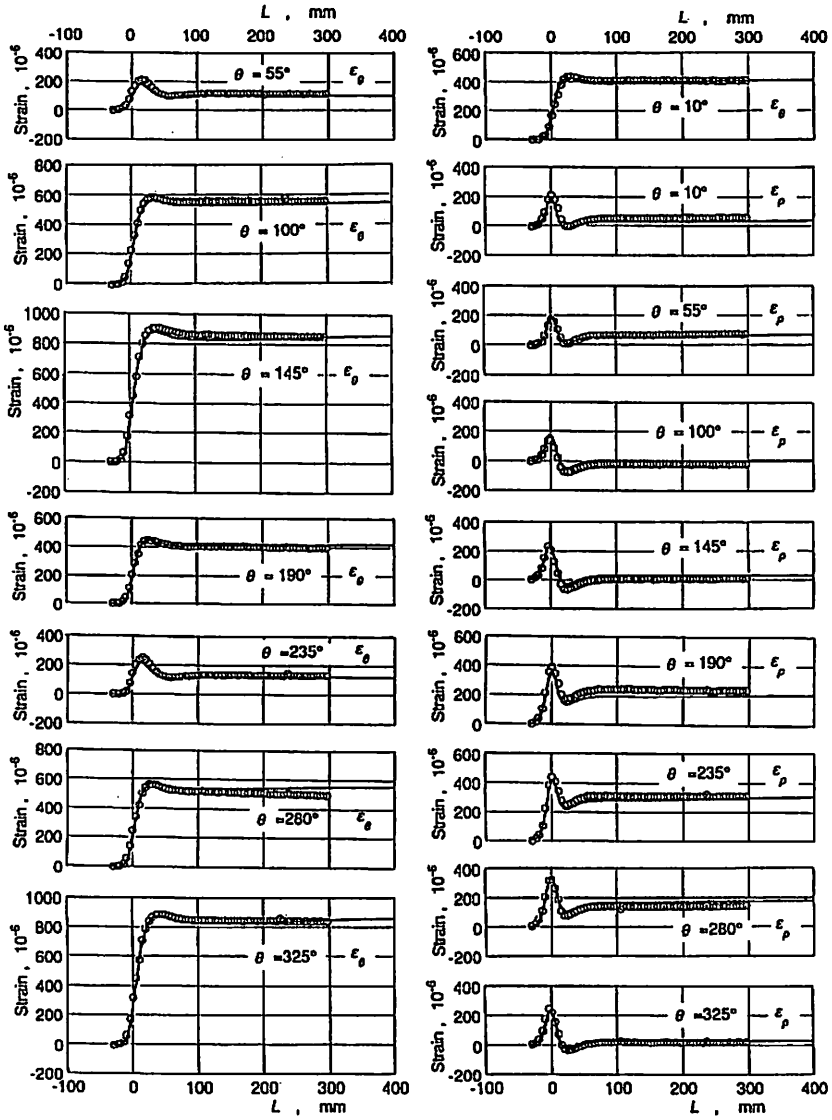

Figure 5 Responses of the strain gauges for every 5mm overcoring advance, comparing to the theoretical curves.

The final strain distribution on the conical socket is shown in **Figure 6**, also comparing to the theoretical curves [11]. The theoretical curves in **Figures 5 and 6** are computed from equation (3), using the stress tensor measured. Good agreement of the theoretical strains with the measured strains demonstrates the reliability of the measurement.

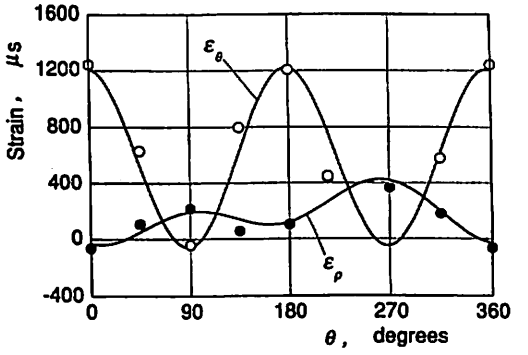

Figure 6 Final strain distribution on the conical socket, comparing to the theoretical curves.

The stress matrix with reference to the (x, y, z) co-ordinates system can be presented. This is useful if a series of measurements are made and the variation is being studied. Alternatively, the principal stress magnitudes and their directions can be presented, both in an isometric plot and/or on a lower hemispherical projection. The isometric plot is demonstrated in **Figure 7 (a)**. This is the result obtained by four times stress measurements using a single horizontal borehole, at the depth of 324 m below the surface, within a vertical pillar of zinc ore, 42 m in width, 100 m in height and 80 m in length [18]. The lower hemispherical projection of the principal stress directions of the case is presented in **Figure 7 (b)**.

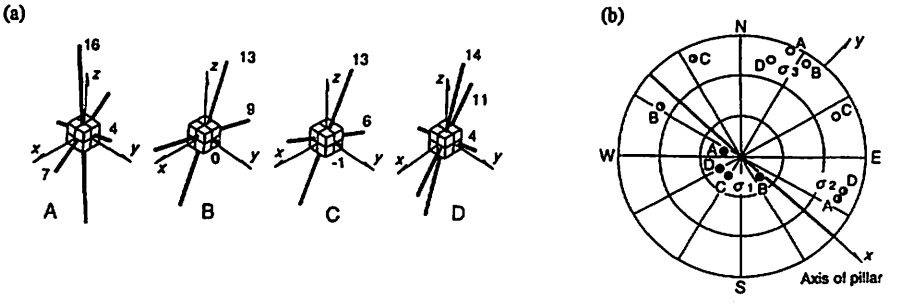

Figure 7 Principal stresses measured in the pillar by four times stress measurement using a borehole; (a) isometric plot, numerals represent the magnitude of the principal stress in MPa; (b) lower hemisphere stereographic projection of the principal direction.

In the case where the stresses are being studied in a specific plane, possibly to correlate with geological feature, it is also available to show the 2-D principal stress magnitudes and directions along the borehole in an appropriate plane. **Figure 8** shows the 2-D principal stress magnitudes and directions along a single borehole, which is drilled horizontally from the wall of a gallery at a depth of 520m in diorite and granodiorite. The borehole intersects with the fault Ⅲ of 0.25m in width dipping about 80 degrees, and an immediate skarn of 1.5m in width [13, 19, 20]. This 2-D expression is useful for understanding the variations of the stress magnitudes and directions along the borehole.

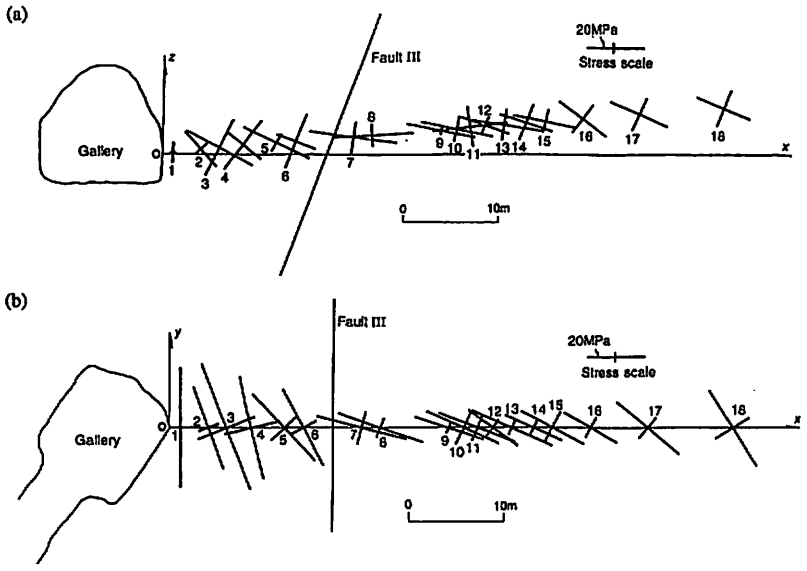

Figure 8 2-D principal stress magnitudes and directions along the borehole in a particular or a specific plane; (a) elevation view; (b) plan view.

When the 24 element strain cell is used, the stress distribution on the borehole socket can be presented, as well as the 3-D *in situ* rock stresses. The principal stress magnitudes and directions on the socket surface can be plotted on the cross sectional view of the borehole [14, 15]. One case is shown in **Figure 9**. The 2-D projection of the surface stress on a conical socket is presented for every overcoring advance, and can be compared with the theory.

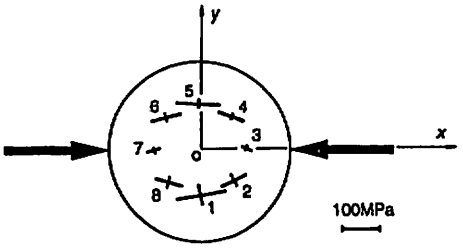

Figure 9 Stress distribution on the conical borehole socket surface, comparing to the maximum compression in the plane perpendicular to the borehole axis (solid arrows).

5. Illustrative Case Example

In situ rock stress measurement by means of the CCBO technique has been conducted in Kamaishi mine, Japan, to evaluate the variation of the regional stress magnitudes, orientations and the stress gradient, including the effect of joints and faults on the stress distribution. **Figure 10** shows the regional principal stress magnitudes and directions in the horizontal planes, evaluated by the multi-times stress measurement and subsequent averaging of each stress component [22, 23].

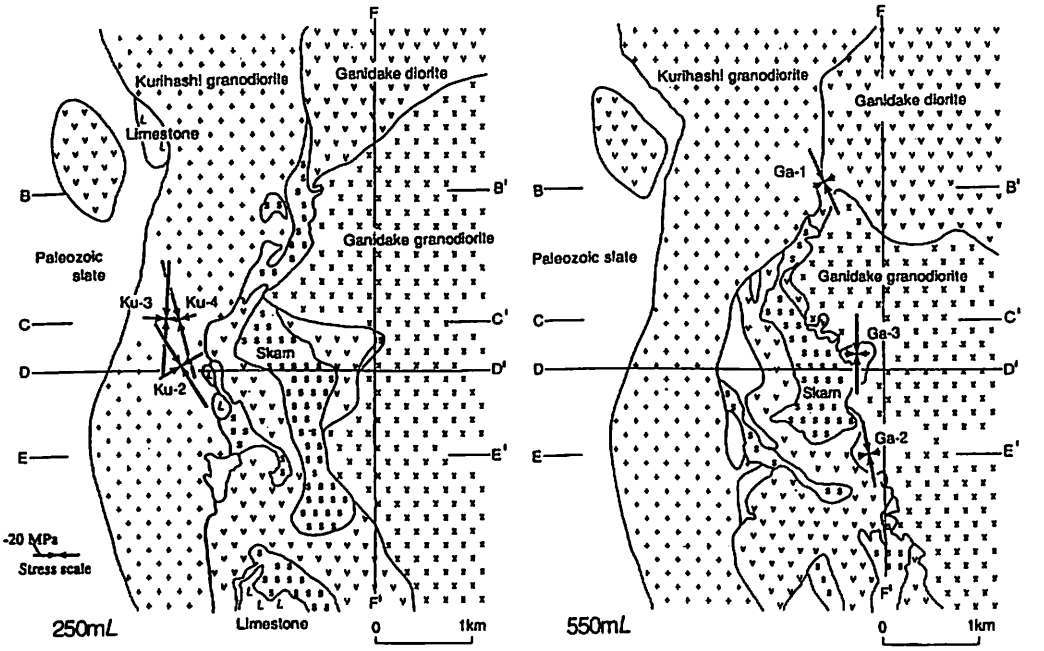

Figure 10 Regional principal stress magnitudes and directions in the horizontal planes, Kamaishi mine, Japan.

Three stations: Ga-1, Ga-2 and Ga-3 have been arranged in Ganidake diorite/granodiorite at +550 m level, and three stations: Ku-1, Ku-2 and Ku-3 are in Kurihashi granodiorite at +250m level. It is noteworthy that the direction of the maximum horizontal compression is approximately in north-south direction and the stress magnitudes increase with increasing the depth below the surface.

At the station Ga-2, the CCBO method has been applied to clarify the effect of joints and faults on the stress distribution [13, 19, 20]. Stresses have been measured 21 times in total in a single borehole in the range from 0.6m to 29.5m apart from the gallery, but the measurement is concluded by giving the 18 reliable results in **Figure 8**. The borehole has intersected not only Fault Ⅲ but also many joints. However, the results obtained clearly indicate that a noteworthy difference of the stress state exists between in front and in the rear of Fault Ⅲ. This means that Fault Ⅲ plays an important role on the stress distribution, while the influence of the joint system is minor.

The time required for the total measurement at the station Ga-2 has been reported to be about 112hours. The time required for each operation has been summarized in **Table 3**, except the time for conventional drilling [20].

Comparison of the CCBO method to other methods has been conducted in several sites in Japan [26, 27]

Table 3 Average time required for the measurement

Operation	Time (minutes)
Creating the conical borehole socket	22.8
Cleaning and the camera operation	10.0
Gluing the strain cell in the place	40.3
Overcoring and strain measurement	22.4
Recovering core with the strain cell	10.4

6. Interpretation of Results

6.1 Determination of elastic moduli

In order to calculate the stress components from the strains, Young's modulus of rock is required as well as Poisson's ratio of rock. For the determination of these two values, the two schemes have been applied. One is a laboratory test using the core sample and the other is *in situ* loading experiment using the conical socket. The former is usually used, and the latter is mainly conducted to re-confirm the reliability of the laboratory test results.

The laboratory test is indispensable to estimate the elasticity, the nonlinearity and the anisotropy of rock. In general, the conventional multi-stage uniaxial compression experiment is conducted. As illustrated in **Figure 11**, three cylindrical specimens of perpendicular to each other, 25mm in diameter and 50mm in length, are taken by drilling the recovered core having a conical socket within. Four cross-typed strain gauges are used to measure the strain response of each specimen. The multi-stage loading pattern is designed to reproduce the axial strain as the same as the maximum strain on the conical socket. The maximum load is usually set lower than 60% of the uniaxial compressive strength of rock. In general, Young's modulus and Poisson's ratio are determined from the linear relation between the axial stress and the strain recovery.

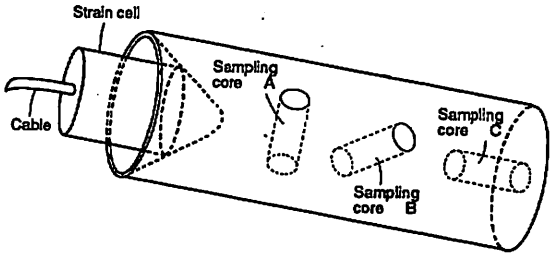

Figure 11 Core sampling for the multi-stage uniaxial compression experiment, in the laboratory.

The *in situ* loading experiment is conducted after gluing the strain cell on a conical socket, just before the commencement of the compact overcoring. As shown in **Figure 12**, a flat-ended ring of 6mm in width is formed, and the axial pressure is applied on it, using a steel ring platen. The pressure-strain relation is monitored, and both Young's modulus and Poisson's ratio of rock are evaluated using the special charts given by the BEM analysis. The procedure has been presented elsewhere [11].

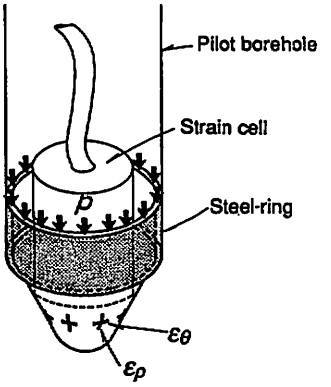

Figure 12 Schematic view of *in situ* axial loading experiment for the determination of elastic moduli.

6.2 Evaluation of rock mass strength

The multi-times CCBO stress measurement is a promising method presently available for the evaluation of the rock mass strength, since it enables one to measure the 3-D stress state within the ground arch and the stress concentration around the cavity. When it is applied to the large rock cavern, such as underground powerhouse caverns, the stress distribution in the ground arch can be measured as well as the stresses within a post failure region neighboring immediately to the cavity face, providing the data closely related to the strength characteristics of rock mass. The strength evaluation based on *in situ* stress measurements is reported in the references [5, 6, 24].

6.3 Evaluation of frictional characteristics of joints

The multi-times CCBO stress measurement is also available for the evaluation of stresses acting on joints and their frictional characteristics. For this purpose, the 3-D stress state is required to be measured at several stations within rock blocks separated by joints. When the joint orientation are determined using the borehole-camera system and/or other methods, the 2-D stresses acting on each joint plane can be estimated from adjacent stress data, applying the stress transformation law. Case examples are reported in the reference [25].

7. Summary and Conclusions

The compact conical-ended borehole overcoring (CCBO) technique is promisingly available for *in situ* rock stress measurement in the faulted and highly jointed rock formations. The apparatus and operating procedure for the CCBO test *in situ* have been described, and the observation equation of the stress tensor to be used in practice has been presented, as well as the recommended procedure for presenting and interpreting the results. Thus, it has been clarified how the three dimensional state of *in situ* rock stress can be determined from the strains on the conical end surface of a single borehole in an isotropic and transversely isotropic rock mass, together with the error in stress. It is remarkable that the overcoring is conducted using the thin walled (3mm) 76mm-diameter bit, which is of the same diameter as the borehole itself. The necessary stress relief is completed by the overcoring advance of 100mm. This is the advantage of the CCBO technique, which enables to measure rock stresses in highly jointed rock formations.

The reliability and the applicability of the CCBO technique have been verified from the case examples. It has been confirmed that the induced stress in a pillar can be measured by the CCBO technique, and that an uniformity of the stress state in the pillar is able to be examined by the reproducibility of the measurements. Namely the same result is obtained more than once by the subsequent measurements. Another case example has shown that the fault dominates the rock stress field, then the stress jump and discontinuity appears along the fault plane. In this case, the 2-D expression of the results is effective for understanding the variations of the stress magnitudes and directions along the borehole. From the last case example, it has been concluded that the multi-times stress measurement by means of the CCBO technique and subsequent averaging of each stress component are effective to evaluate the variation of the regional stress magnitudes, orientations and the stress gradient. Additionally, through interpretation of results, it has been concluded that the CCBO technique is available for both initial and induced rock stress measurements, and also for the evaluation of rock mass strength and the frictional characteristics of joints.

8. Acknowledgments

The authors wish to acknowledge the encouragement and support given by Prof. J.A. Hudson of Imperial College of Science, Technology and Medicine in UK. The authors are also most grateful to Dr. Toshiro Aoki, Tokyu Construction Co. Ltd., Dr. Kiyotoshi Sakaguchi, Research Associate of Tohoku University, Dr. Hyun-Kuk Jang, Messers. Yoshifumi Noguchi and Naoaki Nakamura, Nittetu Mining Co. Ltd., and Dr. Katsuhiko Kaneko, Professor of Hokkaido University for going our research.

References

1. Kim K. and Franklin J.A. Suggested methods for rock stress determination, *Int. J. Rock Mech. Min. Sci. & Geomech. Abstr.* **24** (1), 53-73 (1987).
2. Sugawara K., Obara Y., Okamura H. and Wang Y. The Determination of the Complete State of Stress in Rock by the Measurement of Strains on a Hemispherical Borehole-bottom. *J. Min. Metall. Inst. Japan* **101**, 277-282 (1985).
3. Sugawara K., Obara Y., Okamura H. and Aoki T. Measurement of Strains on a Hemi-spherical Borehole Bottom by the Stress Relief Technique. *J. Min. Metall. Inst. Japan* **102**, 463-468 (1986).
4. Sugawara K., Obara Y., Akimoto M. and Aoki T. Stability Estimation of Large Rock Cavern by In-Situ Stress Measurements. *Proc. Int. Symp. on Engineering in Complex Rock Formations*, Vol. 1, pp.135-141. Beijing (1986).
5. Sugawara K., Kaneko K., Obara Y. and Okamura H. Determination of the State of Stress in Rock by the Measurement of Strains on the Hemispherical Borehole Bottom. *Proc. Int. Symp. Large Rock Cavern*, Vol. 2, pp.1039-1050. Helsinki (1986).
6. Sugawara K., Obara Y., Kaneko K. and Aoki T. Hemispherical-ended Borehole Technique for Measurement of Absolute Rock Stress. *Proc. Int. Symp. Rock Stress and Rock Stress Measurements*, pp.207-216. Stockholm (1986).
7. Sugawara K. and Obara Y. Measurement of *In-Situ* Rock Stress by Hemispherical-ended Borehole Technique. *Int. J. Mining Science and Technology* **3**, 287-300 (1986).
8. Sugawara K., Sakaguchi K., Obara Y., Nakayama T. and Jang H. Rock Stress Measurement and Numerical Approach for Cavern Designing. *J. Korean Rock Mechanics Society* **2** (1), 164-176 (1992).
9. Sakaguchi K., Obara Y., Nakayama T. and Sugawara K. Accuracy of Rock Stress Measurement by means of Conical-ended Borehole Technique. *J. Min. Metall. Inst. Japan* **108**, 455-460 (1992).
10. Nakayama T., Obara Y., Sakaguchi K. and Sugawara K. Conical-ended Borehole Technique for Rock Stress Measurement and its Applications. *Proc. Int. Symp. on Assessment and Prevention of Failure Phenomena in Rock Engineering*, pp.295-300. Istanbul (1993).
11. Sakaguchi K., Takehara T., Obara Y., Nakayama T. and Sugawara K. Rock Stress Measurement by means of the Compact Overcoring Method. *J. Min. Metall. Inst. Japan* **110**, 331-336 (1994).
12. Sakaguchi K., Obara Y., Jang H. and Sugawara K. Process Simulation of Stress Relieving for Rock Stress Measurement. *J. Min. Metall. Inst. Japan* **110**, 601-606 (1994).
13. Sakaguchi K., Jang H., Noguchi Y. and Sugawara K. Application of Conical-ended Borehole Technique to Discontinuous Rock and Consideration. *J. Min. Metall. Inst. Japan* **111**, 283-288 (1995).
14. Obara Y. and Sugawara K. Improvement in Accuracy of the Conical-ended Borehole Technique. *Proc. Int. Symp. on Rock Stress*, pp.77-82. Kumamoto, (1997).
15. Obara Y., Imai K., Nakamura N. and Sugawara K. Improvement of the Conical-ended Borehole Technique for Rock Stress Measurement with a High Accuracy. *J. Min. Metall. Inst. Japan* **113**, 825-831 (1997).
16. Obara Y., Jang H., Murakami K. and Sugawara K. Applicability of the Conical-ended Borehole Technique to Anisotropic Rocks. *J. Min. Metall. Inst. Japan* **111**, 919-924 (1995).
17. Obara Y., Sugawara K., Sakaguchi K. and Mizuochi Y. Application of Hemispherical-ended Borehole Technique to Hot Rock, *Proc. 7th International Congress of ISRM*, pp.587-590.

Aachen (1991).
18. Obara Y., Sugawara K. and Sakaguchi K. Rock Stress Measurements by the Conical-ended Borehole Technique Using the Compact Overcoring. *Proc. 8th International Congress of ISRM*, pp.145-148. Tokyo (1995).
19. Obara Y., Sugawara K. and Takehara T. Rock Stress Measurement by Stress Relieving in Japan. *Proc. MMIJ / AusIMM Joint Symposium '94*, pp.425-432. Ube (1994).
20. Obara Y., Jang H., Sugawara K. and Sakaguchi K. Measurement of Stress Distribution around Fault and Considerations. *Proc. 2nd Int. Conf. on Mechanics of Jointed and Faulted Rock*, pp.495-500. Vienna (1995).
21. Kobayashi S., Nishimura N. and Matumoto K. Displacements and Strains around a Non-flat-end Borehole, *Proc. Int. Symp. of Field measurement in Geomech.*, pp.1079-1084. Kobe (1987).
22. Jang H. and Sugawara K. Macro Rock Stress Measurement at the Kamaishi District. *Proc. the Korea-Japan Joint Symp. on Rock Engineering*, pp.207-215. Seoul (1996).
23. Jang H., Obara Y. and Sugawara K. Rock Stress Measurement in a Granitic Massif by means of the Conical-ended Borehole Technique. *Proc. Int. Forum of Resources Engineering*, pp. pp.256-261. Seoul (1994).
24. Obara Y. and Sugawara K. Field Stress Measurements in Jointed Rock. *Proc. Int. Conf. on Mechanics of Jointed and Faulted Rock*, pp.827-834. Vienna (1990).
25. Sugawara K. Initial Stress. *Mechanics of Rock*, pp.357-383. Maruzen, Tokyo (1993).
26. Denboya N., Fukuhara A., Obara Y. and Sugawara K. Applicability of the Compact Overcoring Method for Initial Stress Measurement in Highly Cracked Bedrock. *Proc. Int. Symp. on Rock Stress*, pp.83-88. Kumamoto (1997).
27. Ishiguro Y., Nishimura H., Nishino K. and Sugawara K. Rock Stress Measurement for Design of Underground Powerhouse and Considerations. *Proc. Int. Symp. on Rock Stress*, pp.491-498. Kumamoto (1997).